Comparison between simulated observational and true radial profiles for FIRE-2 galaxies

Dennis Raush, Shea Garrison-Kimmel, Suoqing Ji, Philip Hopkins

Introduction

Measuring how the amount of light emitted from a galaxy varies with the distance from its center (i.e. its light profile) is one of the best ways we can understand both individual galaxies and galaxy populations as a whole. These measurements can help categorize galaxies by their types (e.g. elliptical, spheroidal, or spiral), ages, and masses. One of the standard ways to approximate the light curve of a galaxy is using a Sersic exponential function fit [1]. In this paper, we analyze the accuracy of Sersic fits of simulated light profiles for galaxies of different sizes, observed in different bands at varying inclinations, in estimating the radius at which half of the galaxy's mass is contained ($R_{1/2}$) using a set of 21 simulated galaxies from the FIRE-2 simulation suite [2].

Methods

Source data

The source data for this work is from the FIRE-2 simulations [2], run using the GIZMO simulation package [3]. Gizmo is a state-of-the-art multi-physics simulation suite including calculations accounting for radiation pressure, stellar mass loss, photo-ionization and photo-heating, supernovae, and much more. The physics used in the FIRE-2 simulations is identical to that used for FIRE-1 [4], but the source code was modified to incorporate some bug fixes and numerical improvements.

Each FIRE-2 simulation snapshot is a set of unique IDs, 3D coordinates, velocities, masses, and other properties for a large number of "particles at a given time", each representing either baryonic matter (gas or stars) or dark matter, and together forming a "representative" part of the Universe, in which most of the particles end up in a single model of a galaxy or galaxy system. Star and gas particles have additional information: both of them have "metallicities" (fraction of the particle's mass in elements other than hydrogen), and star particles have information regarding the age of the star. Gas particles also track internal energy, density, spatial extent, electron abundance, neutral hydrogen abundance, and instantaneous rate at which stars are forming out of that gas at that snapshot [2]. Table 1 lists the galaxies we studied in this paper, along with their resolution levels, halo mass, effective radius, and simulation class.

A representative example, m12i_res7100, contained 13,976,485 particles of type "star", each with initial mass of ~7,000 Msun because it is a high-resolution "Latte" suite simulation [5], with the final "star" particle mass of ~5,000 Msun due to stellar mass loss. The total number of particles in the m12i_res7100 halo is ~140 million, and the mass of each dark matter particle is 43,000 Msun i.e. about 5 times larger than that of each baryonic particle, in accordance with the universal baryon fraction [2].

Calculation of galaxy properties

The following galaxy properties were calculated directly from the snapshots using the *utilties.particle.get_galaxy_properties()* function from Dr. Andrew Wetzel's *utilities* library https://bitbucket.org/awetzel/utilities/src/master/):

- Radius_90_3D and Mass_90_3D - radius within which 90% of the stellar mass of the galaxy is contained, in kpc, and the respective mass, in Msun

- Radius_50_3D and Mass_50_3D - radius within which 50% of the stellar mass of the galaxy is contained, in kpc, and the respective mass, in Msun
- Radius_90_2D and Mass_90_2D - radius within which 90% of the stellar mass of the galaxy is contained, in kpc, and the respective mass, in Msun, calculated using only the major axis
- Radius_50_2D and Mass_50_2D - radius within which 50% of the stellar mass of the galaxy is contained, in kpc, and the respective mass, in Msun, calculated using only the major axis

Additionally, Radius_halo and Mass_halo were calculated, representing virial mass and virial radius of the main halo, using *utilties.particle.get_halo_properties()*.

Values can be found in Table 1 and Supp Figure 1.

Generation of simulated observational galaxy light profiles from FIRE-2 data

All analysis was conducted using *python3*, primarily the *numpy* [6], *matplotlib* [7], *scipy* [8], *pandas* [9], and *gizmo_analysis* (https://bitbucket.org/awetzel/gizmo_analysis/src/master/) modules.

We take 3D coordinates and bolometric, infrared, and ultraviolet intensities (Bol, I, and U bands) of all particles of type “star” in the given galaxy.

Using Andrew Wetzel’s *utilities* package, we rotate and translate the galaxy so that its center is at the origin and the z-axis is aligned with the line-of-sight at inclinations ranging from 0° to 90°, in increments of 30° (*utilities.coordinate.get_coordinates_rotated()*). The inclination of 0° corresponds to a face-on view of the galaxy (as returned by *utilities.particle_get_distance_wrt_center()*). After this, the z-coordinates of all particles are discarded and the x- and y-coordinates are treated as 2D projections at the given inclination.

Next, we create 29 annuli with radii equally spaced on a log scale from 0.1 kpc to 30 kpc (i.e. the inner radius of the smallest annulus is 0.1 kpc, and the outer radius of the largest annulus is 30 kpc; these boundaries were adjusted for the 7 smallest galaxies). The total luminosity of all particles within each annulus is then calculated and divided by the annulus area to calculate density. The calculated density profiles are given in Supp Figure 2.

Code is given below:

```
def radial_profile(a, b, val, bins=30):
      # a, b are numpy.ndarrays of abscissae and ordinates of all star-type
      particles in the simulation, viewed at the given angle
      # val is the numpy.ndarray of their luminosities in the given band, or
      masses - whatever we are binning

    if np.isscalar(bins):
        assert int(bins) == bins
        bins = np.logspace(-1, np.log10(30), int(bins))
      # (0.1, 0.1217, 0.148, … , 20.24, 24.64, 30.)

    bins_mid = 10**(0.5*(np.log10(bins[:-1])+np.log10(bins[1:])))

    dist = np.sqrt(a**2 + b**2) # numpy.ndarray of distances to the origin

    result = np.zeros(bins.size - 1)
    for ii, dmin in enumerate(bins[:-1]):
```

```
        dmax = bins[ii+1]
        msk = (dist >= dmin) & (dist < dmax) # a numpy.ndarray of trues and
falses
        totval = val[msk].sum() #... which can be applied to val to get a sum of
selected values
        area = np.pi * (dmax**2 - dmin**2) # area of the annulus
        result[ii] = totval/area # density for the given annulus
    return bins, bins_mid, result, totval, area
```

Generation of galaxy mass profiles from FIRE-2 data

We take 3D coordinates and masses of all particles of type "star" in the given galaxy. The rest of the procedure is identical to the generation of galaxy light profiles described above.

Calculation of Sersic fits and parameters for the simulated observational galaxy light profiles

For each light profile (3 bands x 4 inclinations x 21 galaxies), we calculated a Sersic fit that is defined by 3 numbers: effective radius R_e (also called $R_{1/2}$), intensity at that radius, I_e, and Sersic index, *n*. The Sersic fit formula that we used is $I(R) = I_e\, e^{b_n(1-\frac{R}{R_e}^{1/n})}$, where $b_n(n) = 2n - \frac{1}{3} + \frac{4}{405n} + \frac{46}{25515n^2}$[10]. Best values for the three parameters (R_e, I_e, and *n*) were determined using the *optimize_curve_fit()* function from the *scipy* library, with the algorithm set as *dogbox* and limits on Sersic index as $0 < n < 15$. We limited the Sersic index to ensure that the algorithm converges to reasonable values for all input light profiles. Without the upper limit, we would get fits that fail to represent the raw values. The obtained parameters are reported in Supp. Table 1 and fits in Supp. Figures 3-6.

The R_e (or $R_{1/2}$) determined by this procedure are "simulated observational" values. They were compared to the true $R_{1/2}$ for each galaxy, as determined from its mass profiles. Data was plotted and organized using *matplotlib*.

Results

By relying on light profiles, $R_{1/2}$ of galaxies in binary systems is consistently overestimated

Following estimation of $R_{1/2}$ for the galaxies at different inclinations and in different bands using Sersic fits, we plotted these values against the true $R_{1/2}$ calculated directly from mass profiles at respective inclinations. The obtained results are shown in Figure 1. We see that for 15 of 21 galaxies, the simulated observational $R_{1/2}$ correlates with true $R_{1/2}$ and closely matches it at inclination angle = 0. However, it is clear that for galaxies with a close neighbor, as in the case of our galaxy (the Milky Way) with Andromeda (M31), $R_{1/2}$ calculated from the simulated observational data (light profiles) is much larger than their true $R_{1/2}$ at every inclination. In addition to the binary galaxies, galaxy m12f exhibits the same problem. This phenomenon is interesting because the accuracy of the observational $R_{1/2}$ does not appear dependent on any other galaxy property such as galaxy size or mass: for example, there are massive galaxies for which observational $R_{1/2}$ is essentially equal to true $R_{1/2}$, such as m12m at inclination = 0. Supp. Fig 7 shows that there is no distinct relationship between galaxy mass and simulated observational $R_{1/2}$.

For galaxies whose mass profiles are not "parallel" to light profiles, the simulated observational $R_{1/2}$ is consistently wrong

Next we asked the question: why are binary galaxies and m12f consistently overestimated in their simulated observational $R_{1/2}$, but other galaxies are not? To gain more insight into this problem, we analyzed the mass and light radial profiles for each galaxy (Supp. Figures 3-6). We noticed that for problematic galaxies, there is a significant difference between the slope of the mass profile and light profiles, while for the other galaxies, the difference is much less prominent. For example, for m12i, a normal, non-problematic galaxy, the mass profile is essentially parallel to the slopes of its light profiles in different bands (Figure 2). On the other hand, m12f, a "problematic" galaxy, shows a positive difference between the slopes of its mass profiles and light profiles, which explains why the $R_{1/2}$ estimated by light is much larger than true $R_{1/2}$ estimated through mass (Figure 3). An opposite example is given by m11d, whose mass profile is much flatter than its light profiles, meaning that it underestimates $R_{1/2}$ at large inclinations (Supp. Figure 6).

Light profiles of problematic galaxies tend to be flatter than others

We also noticed that for problematic galaxies, all of their light profiles are flatter than the others. For Sersic fits, flatter profiles mean higher Sersic indices. We believe that the cause of this might be that the bounds used when calculating the binned light profiles failed to encompass a sufficiently broad range of distances from the galaxy center, instead representing only a small portion of the galaxy's stellar distribution. Supp. Figure 8 shows that there is no distinct relationship between galaxy stellar mass and Sersic index. Interestingly, lower Sersic indices (more concave light profile) always lead to fairly accurate predicted $R_{1/2}$, whereas higher Sersic indices (flatter light profile) often lead to predictions being off by as high as a factor of 9 (Supp. Figure 9). An interesting observation is that $R_{1/2}$ estimated from infrared (I-band) light profiles tend to be less inaccurate than those in ultraviolet (U-band) and bolometric (Bol-band) (Supp. Figure 9).

At larger inclination, $R_{1/2}$ is more likely to be underestimated

Another phenomenon we noticed was that as inclination increases, the $R_{1/2}$ calculated through light profiles becomes smaller. For example, for m12i, the simulated observational $R_{1/2}$ values calculated by Sersic-fitting Bol light profiles for inclination angles of 0, 30, 60, and 90, are 3.37 kpc, 3.21 kpc, 2.82 kpc, and 2.27 kpc, respectively (true $R_{1/2}$ of 2.53 kpc). This is because the observational $R_{1/2}$ is calculated from light emitted per area - when area decreases (as the inclination angle increases), the observed intensity of light becomes less accurate.

Discussion/Conclusion

In our study, we found that for a subset of galaxies, observationally derived Sersic fits work surprisingly well at low inclination (close to face-on). We also noticed that for galaxies with "flatter" light profiles (meaning higher Sersic index), the simulated observation $R_{1/2}$ is consistently overestimated. Further study of the relationship between galaxy morphology and flatness of the light profile would be required to make more definite conclusions on why this occurs. An important caveat in our study is that we did not include dust obscuration. Even without dust obscuration, we see that light profile predictions underestimate $R_{1/2}$ at high inclinations. We predict that this effect would be aggravated in the presence of dust obscuration.

Bibliography

1. Sérsic, J.L., *Influence of the atmospheric and instrumental dispersion on the brightness distribution in a galaxy.* Boletin de la Asociacion Argentina de Astronomia La Plata Argentina, 1963. **6**: p. 41.
2. Hopkins, P.F., et al., *FIRE-2 simulations: physics versus numerics in galaxy formation.* Monthly Notices of the Royal Astronomical Society, 2018. **480**(1): p. 800-863.
3. Hopkins, P.F., *A new class of accurate, mesh-free hydrodynamic simulation methods.* Monthly Notices of the Royal Astronomical Society, 2015. **450**(1): p. 53-110.
4. Hopkins, P.F., et al., *Galaxies on FIRE (Feedback In Realistic Environments): stellar feedback explains cosmologically inefficient star formation.* Monthly Notices of the Royal Astronomical Society, 2014. **445**(1): p. 581-603.
5. Wetzel, A.R., et al., *Reconciling dwarf galaxies with λCDM cosmology: simulating a realistic population of satellites around a Milky Way-mass galaxy.* The Astrophysical Journal, 2016. **827**(2): p. L23.
6. van der Walt, S., S.C. Colbert, and G. Varoquaux, *The NumPy Array: A Structure for Efficient Numerical Computation.* Computing in Science & Engineering, 2011. **13**(2): p. 22-30.
7. Hunter, J.D., *Matplotlib: A 2D Graphics Environment.* Computing in Science & Engineering, 2007. **9**(3): p. 90-95.
8. Oliphant, T.E., *Python for Scientific Computing.* Computing in Science & Engineering, 2007. **9**(3): p. 10-20.
9. McKinney, W. *Data Structures for Statistical Computing in Python*. in *9th Python in Science*. 2010.
10. Ciotti, L. and G. Bertin, *Analytical properties of the R^1/m law.* Astronomy and Astrophysics, 1999. **352**: p. 447-451.

Figures and tables

Table 1. The 21 FIRE-2 simulation galaxies studied here.

Name	mi, $1000M_{Sun}$	M_{halo}, M_{Sun}	R_{halo}, kpc	Simulation class	Notes[2]
m10q	0.03	8.24×10^{09}	64.18	Low-mass dwarf (M_{halo}~$10^{10}M_{Sun}$)	
m11b	0.26	4.45×10^{10}	112.59	Intermediate-mass dwarfs ($10^{10}M_{Sun}<M_{halo}<10^{12}M_{Sun}$)	
m11i	7.1	7.77×10^{10}	132.61	Intermediate-mass dwarfs ($10^{10}M_{Sun}<M_{halo}<10^{12}M_{Sun}$)	
m11q	0.88	1.63×10^{11}	173.74	Intermediate-mass dwarfs ($10^{10}M_{Sun}<M_{halo}<10^{12}M_{Sun}$)	Early-forming, large core
m11e	7.1	1.68×10^{11}	171.32	Intermediate-mass dwarfs ($10^{10}M_{Sun}<M_{halo}<10^{12}M_{Sun}$)	
m11h	0.88	1.86×10^{11}	177.37	Intermediate-mass dwarfs ($10^{10}M_{Sun}<M_{halo}<10^{12}M_{Sun}$)	
m11d	7.1	3.23×10^{11}	213.14	Intermediate-mass dwarfs ($10^{10}M_{Sun}<M_{halo}<10^{12}M_{Sun}$)	
m12z	4.2	9.25×10^{11}	307.42	Milky Way-mass 'latte' haloes (M_{halo}~$10^{12}M_{Sun}$)	
m12w	7.1	1.08×10^{12}	318.50	Milky Way-mass 'latte' haloes (M_{halo}~$10^{12}M_{Sun}$)	
m12r	7.1	1.10×10^{12}	321.08	Milky Way-mass 'latte' haloes (M_{halo}~$10^{12}M_{Sun}$)	
m12i	7.1	1.18×10^{12}	335.78	Milky Way-mass 'latte' haloes (M_{halo}~$10^{12}M_{Sun}$)	Latte' primary halo
m12c	7.1	1.35×10^{12}	351.45	Milky Way-mass 'latte' haloes (M_{halo}~$10^{12}M_{Sun}$)	
m12b	7.1	1.43×10^{12}	358.36	Milky Way-mass 'latte' haloes (M_{halo}~$10^{12}M_{Sun}$)	
m12m	7.1	1.58×10^{12}	370.52	Milky Way-mass 'latte' haloes (M_{halo}~$10^{12}M_{Sun}$)	Earlier forming halo, boxy bulge
m12f	7.1	1.71×10^{12}	380.00	Milky Way-mass 'latte' haloes (M_{halo}~$10^{12}M_{Sun}$)	MW-like halo
Juliet	3.5	1.10×10^{12}	321.23	MW-like in Local Group pair	
Romeo	3.5	1.32×10^{12}	340.90	M31-like in Local Group pair	
Louise	4	1.15×10^{12}	333.17	MW-like in Local Group pair	
Thelma	4	1.43×10^{12}	358.23	M31-like in Local Group pair	
Remus	4	1.22×10^{12}	339.15	MW-like in Local Group pair	
Romulus	4	2.08×10^{12}	405.62	M31-like in Local Group pair	

Figure 1.

Scatter plots of true $R_{1/2}$ calculated from mass profiles (horizontal) against simulated observational $R_{1/2}$ determined by Sersic fits of light profiles in different bands at inclinations of 0, 30, 60, and 90 degrees (vertical). Each galaxy is represented by three data points, connected by a gray vertical line. These points are the simulated observational $R_{1/2}$ for the I, Bol, and U bands. The black line represents y = x, or perfect match.

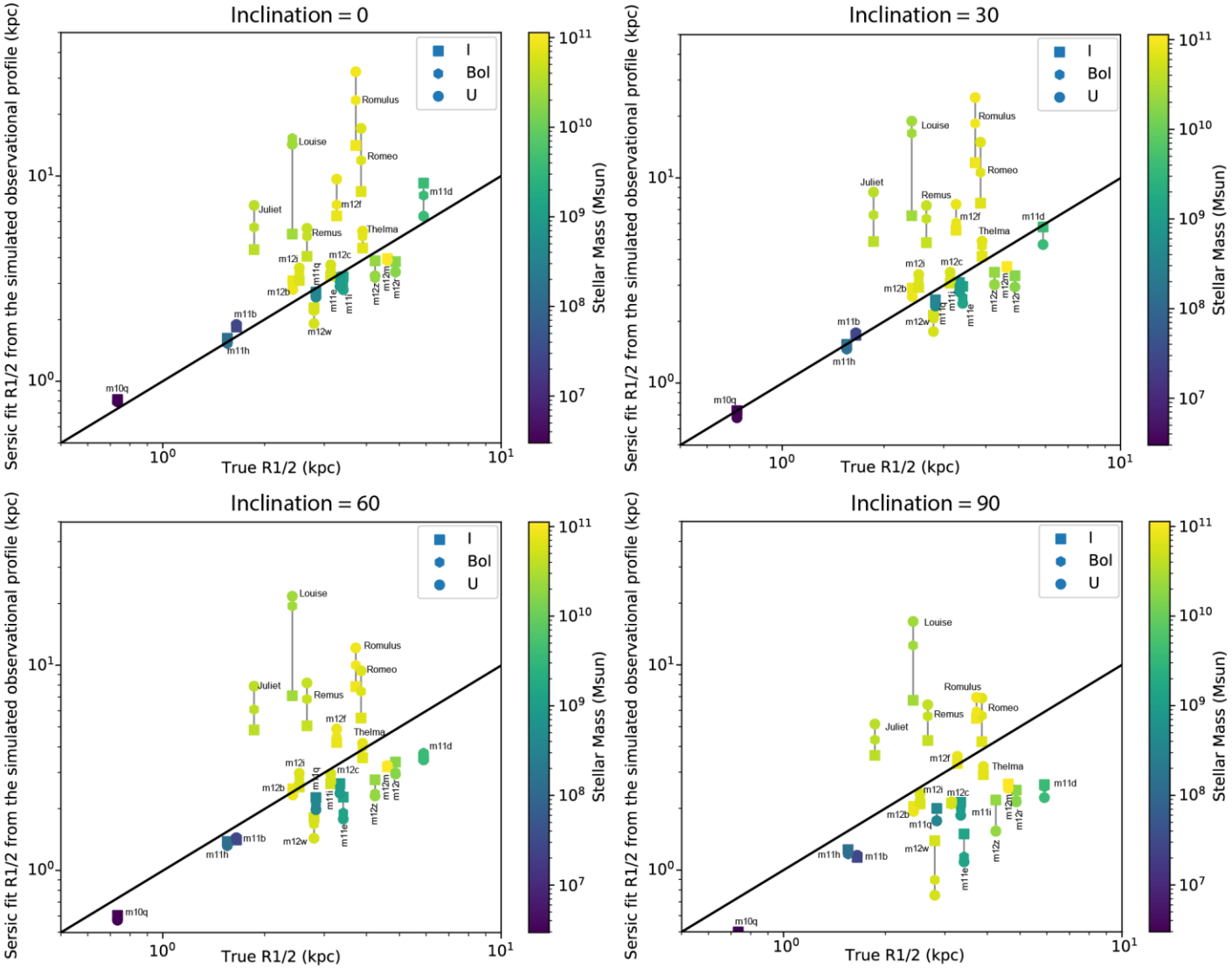

Figure 2.

Comparison of structure and radial profiles at inclinations 0 (face-on) and 90 (edge-on) for galaxy m12i. Top row: Particle plot of the bolometric light density of m12i next to its mass profile and light profiles in U, I, and Bol for a face-on view. Bottom row: Particle plot of the bolometric light density of m12i next to its mass profile and light profiles in U, I, and Bol for a edge-on view. Note that the slope of the mass profiles matches that of the light profiles for both face-on and edge-on views - this results in a fairly accurate estimate of the true $R_{1/2}$ from the Sersic fits of the light profiles in all three bands.

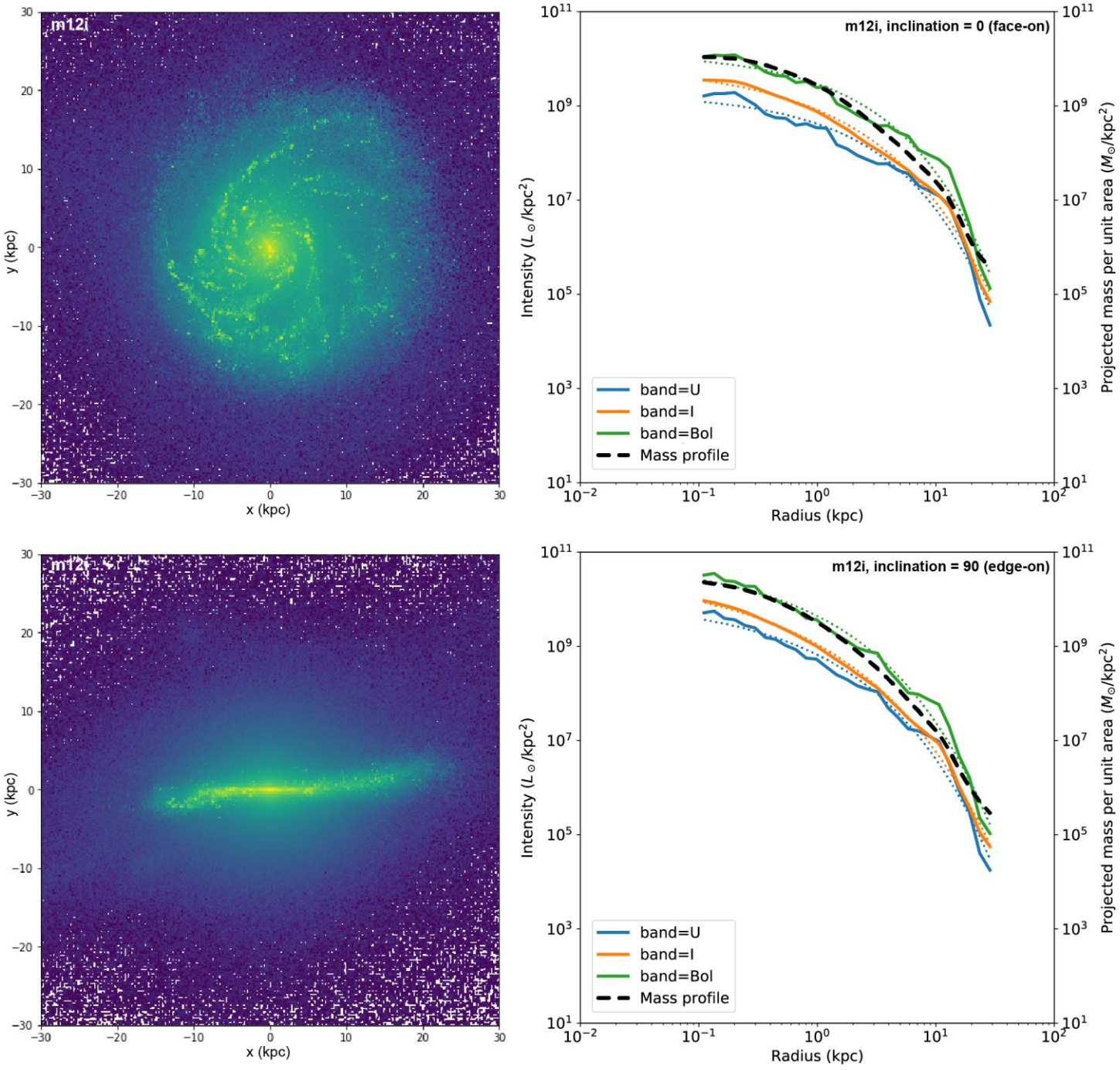

Figure 3.

Comparison of structure and radial profiles at inclinations 0 (face-on) and 90 (edge-on) for galaxy m12f. Top row: Particle plot of the bolometric light density of m12f next to its mass profile and light profiles in U, I, and Bol for a face-on view. Bottom row: Particle plot of the bolometric light density of m12f next to its mass profile and light profiles in U, I, and Bol for a edge-on view. Note for the face-on view, the mass profile slope is much steeper than the slopes of either of the three light profiles. This results in an inaccurate estimate of the true $R_{1/2}$ from the Sersic fits of the light profiles in all three bands at inclination 0.

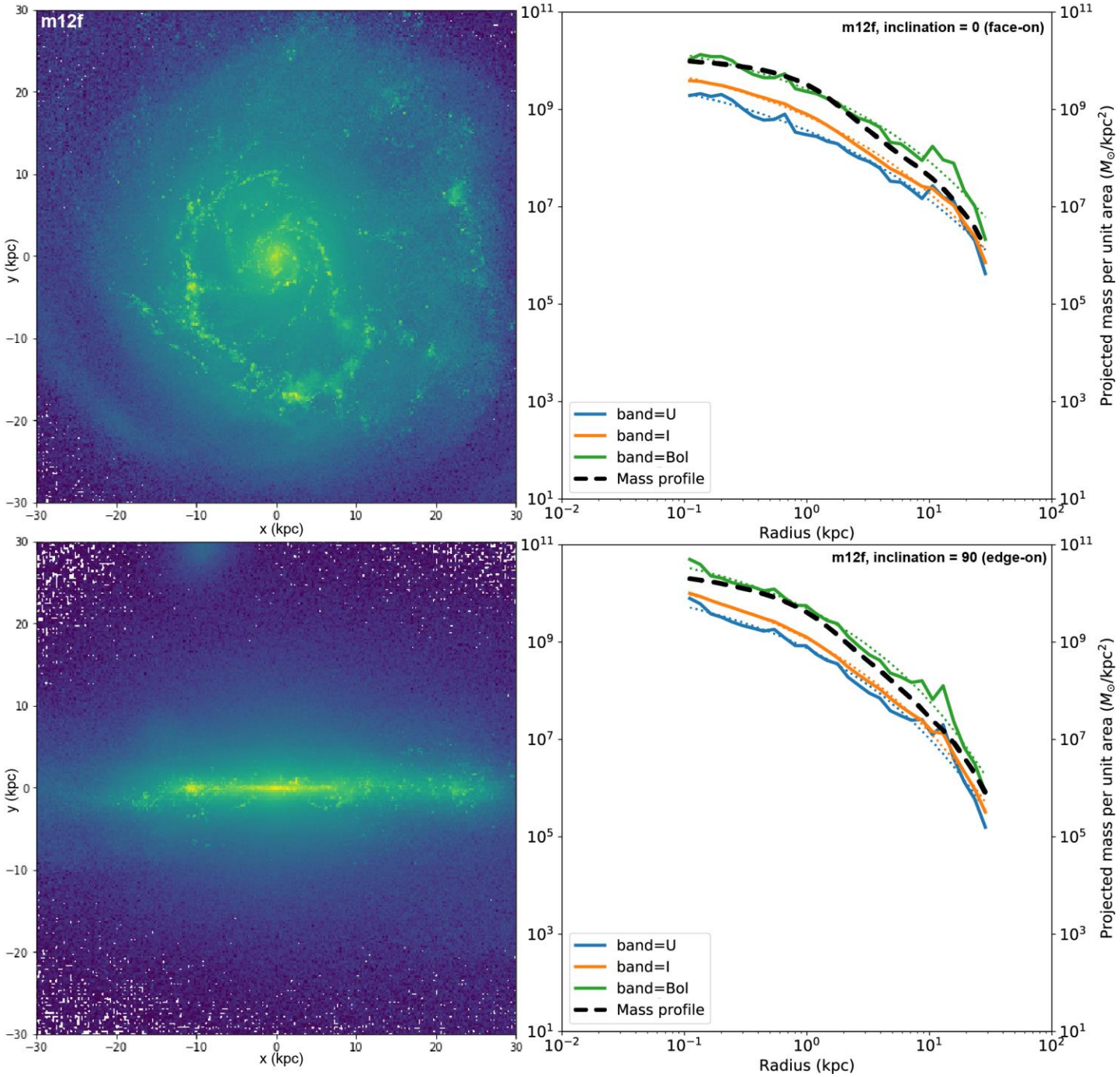

Supp. Table 1 (spreadsheet). Computed parameters for the 21 FIRE-2 galaxies in this work.

Supp. Figure 1. Calculated masses of each of the 21 galaxy halos studied in this paper.
(A) Masses shown as a bar graph. There are four distinct categories of galaxy type when comparing the masses, represented by color (see also Table 1). We separated the galaxies into sub-Milky Way-mass galaxies (i.e. "dwarfs," in green), Milky Way-mass galaxies with a nearby neighbor (i.e. systems that mimic the Milky Way and M31 configuration, in red), and isolated Milky Way-mass galaxies (purple).
(B) Scatter plot of halo mass against 90% stellar mass for the 21 galaxies studied.

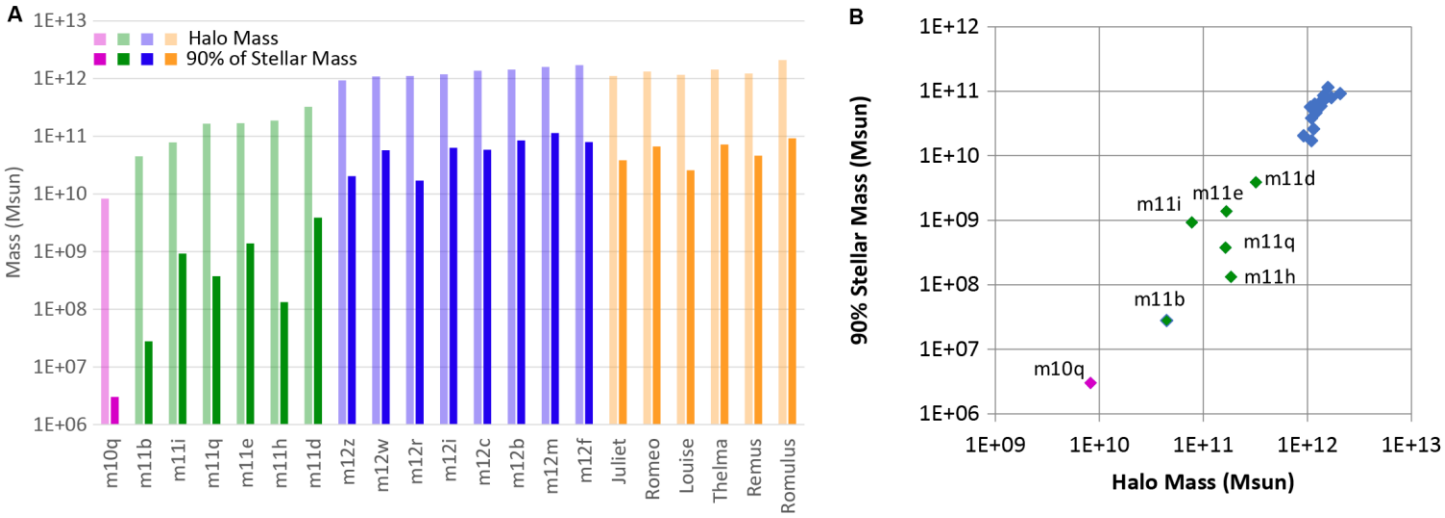

Supp. Figure 2.

Mass profiles of all the galaxies in this paper. The profiles are calculated similarly to light density, meaning that the mass in each annulus in the given 2D projection is divided by the area of that annulus. This is why there are small variations in mass profiles between different inclinations.

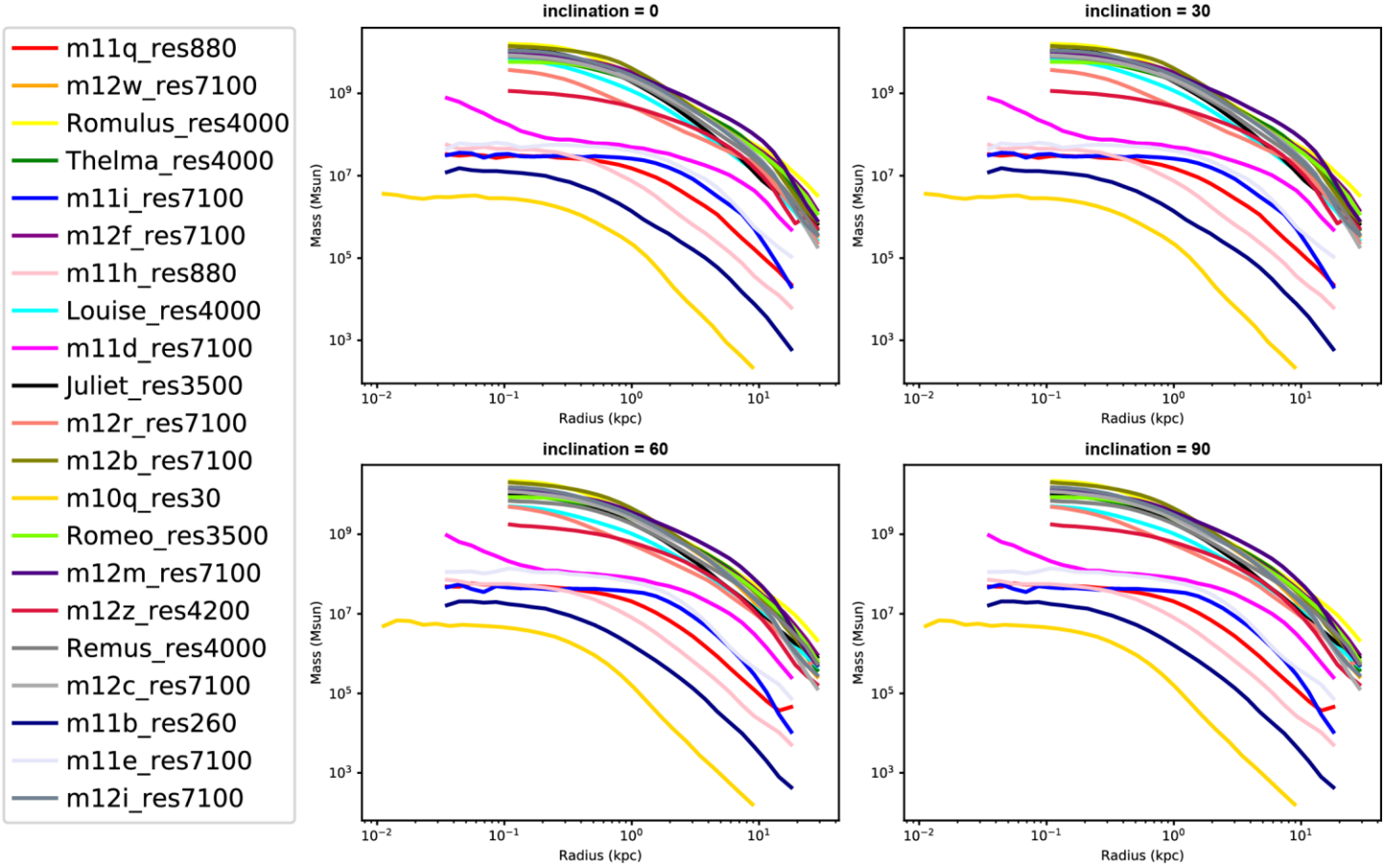

Supp. Figure 3.

Mass and light profiles for each for each of the 21 galaxies in this paper at an inclination of 0 degrees. Solid colored lines indicate the light profiles from each simulation, while colored dotted lines correspond to the Sersic fit for the profile. The grey dashed line indicates the mass profile.

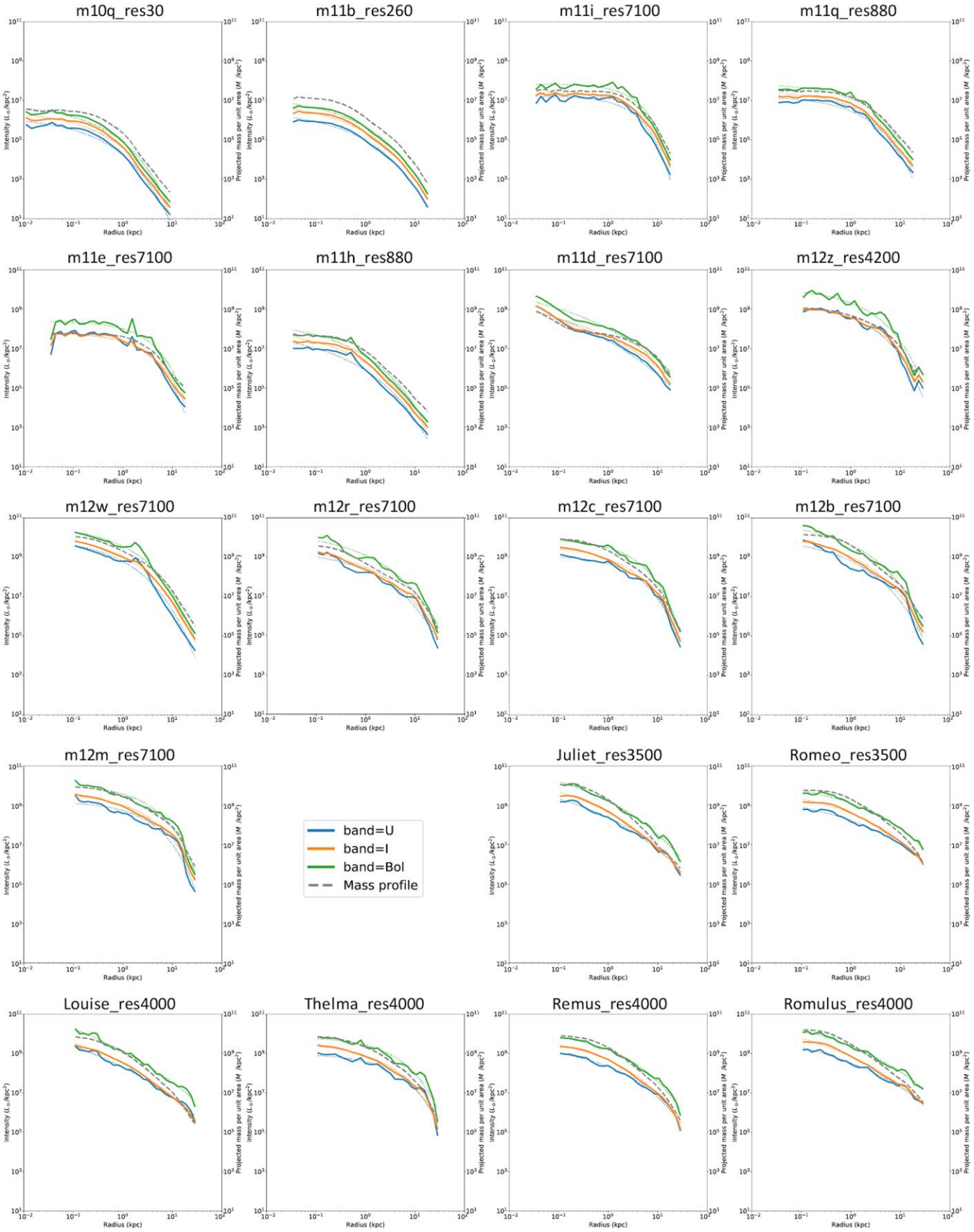

Supp. Figure 4.

Mass and light profiles for each for each of the 21 galaxies in this paper at an inclination of 30 degrees. Solid colored lines indicate the light profiles from each simulation, while colored dotted lines correspond to the Sersic fit for the profile. The grey dashed line indicates the mass profile.

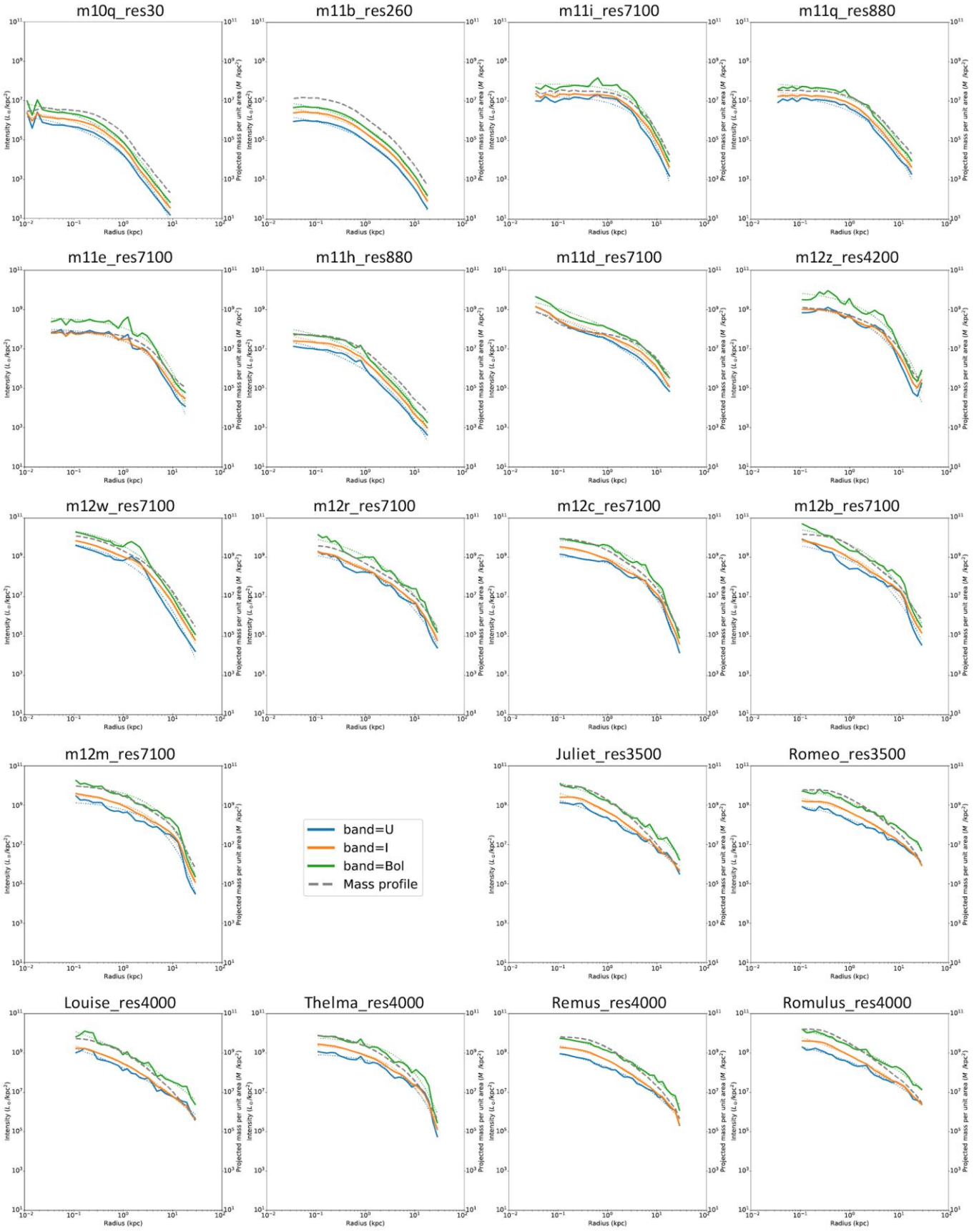

Supp. Figure 5.

Mass and light profiles for each for each of the 21 galaxies in this paper at an inclination of 60 degrees. Solid colored lines indicate the light profiles from each simulation, while colored dotted lines correspond to the Sersic fit for the profile. The grey dashed line indicates the mass profile.

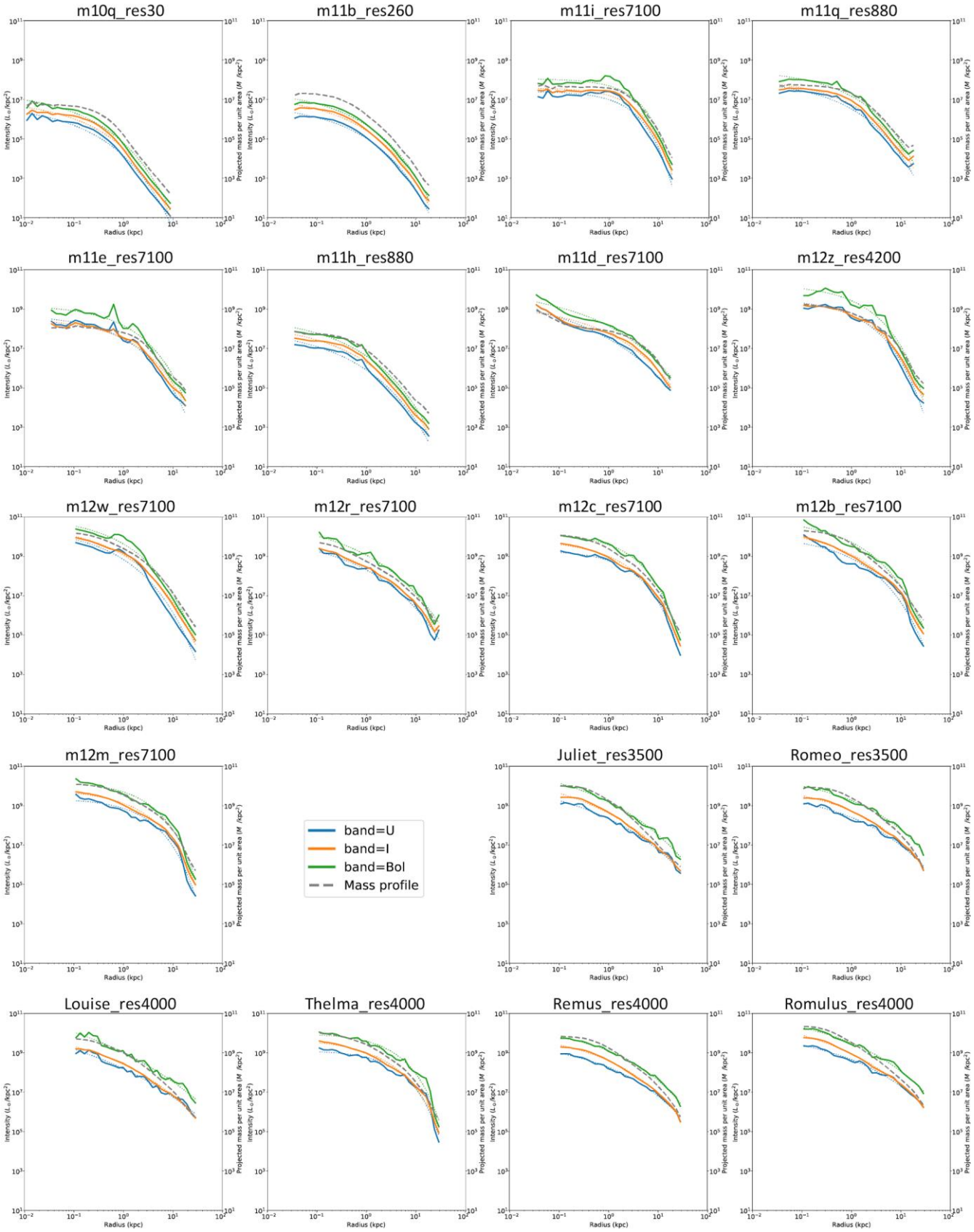

Supp. Figure 6.

Mass and light profiles for each for each of the 21 galaxies in this paper at an inclination of 90 degrees. Solid colored lines indicate the light profiles from each simulation, while colored dotted lines correspond to the Sersic fit for the profile. The grey dashed line indicates the mass profile.

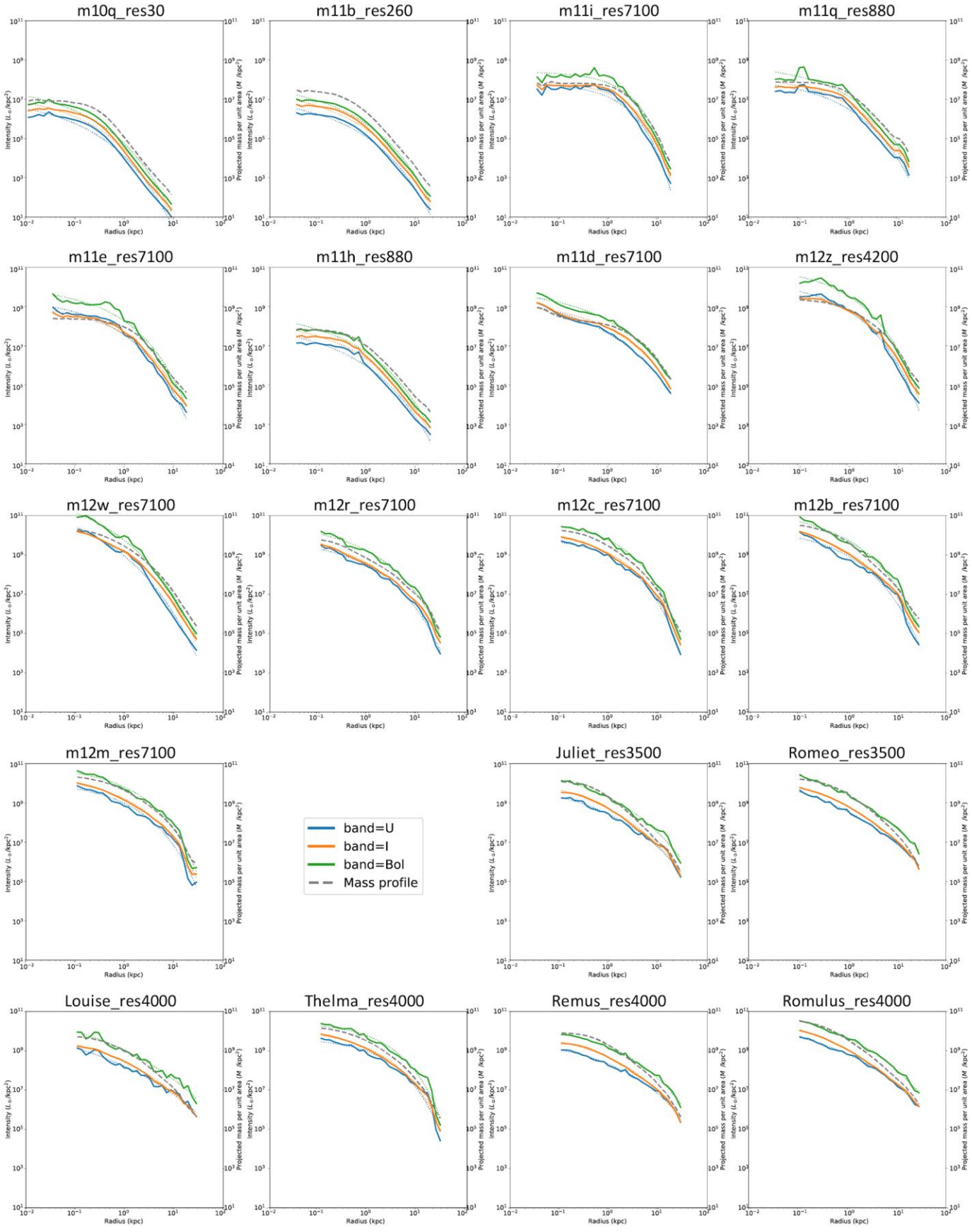

Supp Figure 7.

Scatter plots of 90% stellar mass (horizontal) against simulated observational $R_{1/2}$ determined by Sersic fits of light profiles in different bands at inclinations of 0, 30, 60, and 90 degrees (vertical). Each galaxy is represented by three data points, connected by a gray vertical line. These points are the simulated observational $R_{1/2}$ for the I, Bol, and U bands.

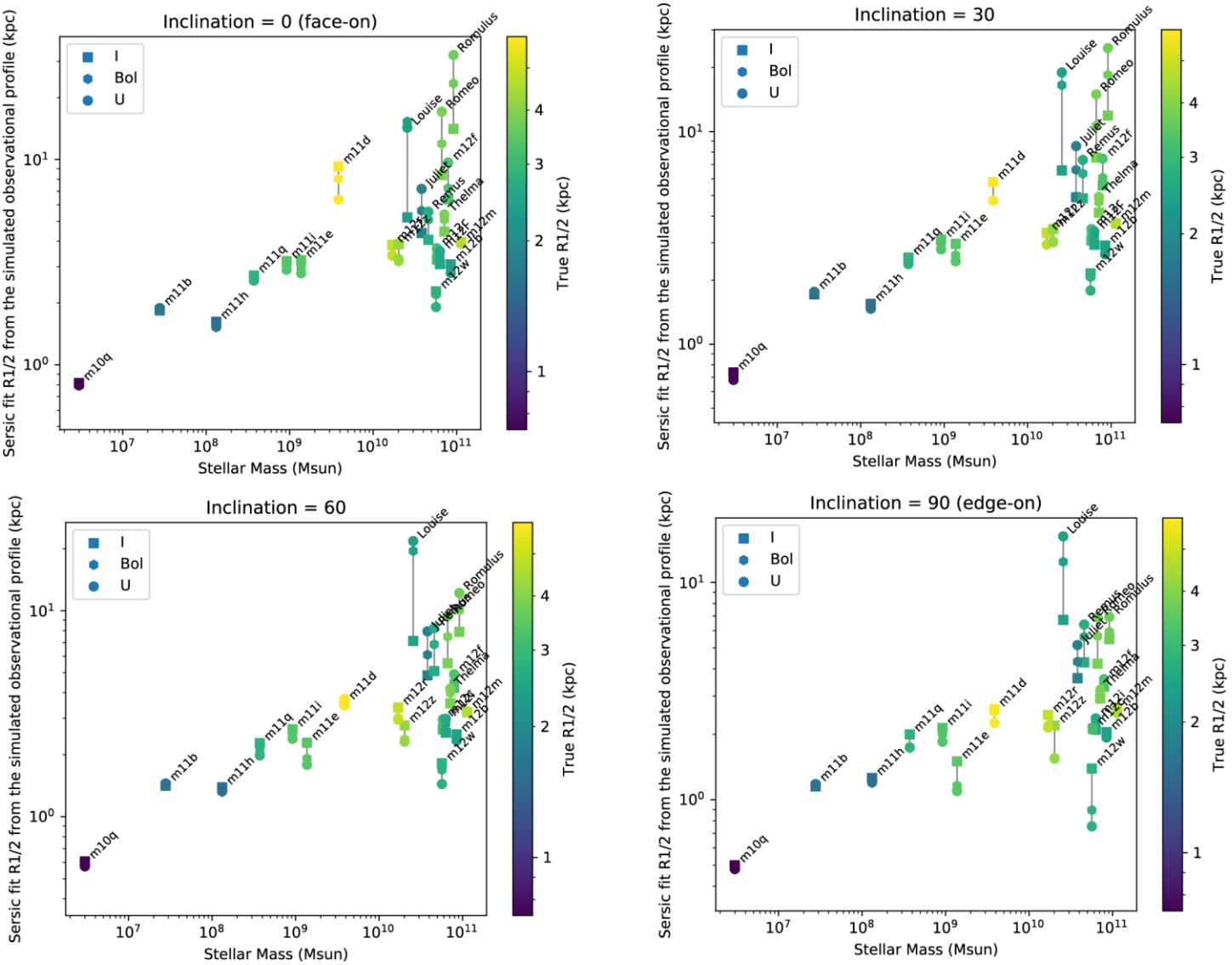

Supp Figure 8.

Scatter plots of 90% stellar mass (horizontal) against Sersic index at inclinations of 0, 30, 60, and 90 degrees (vertical). Each galaxy is represented by three data points, connected by a gray vertical line. These points are the simulated observational $R_{1/2}$ for the I, Bol, and U bands.

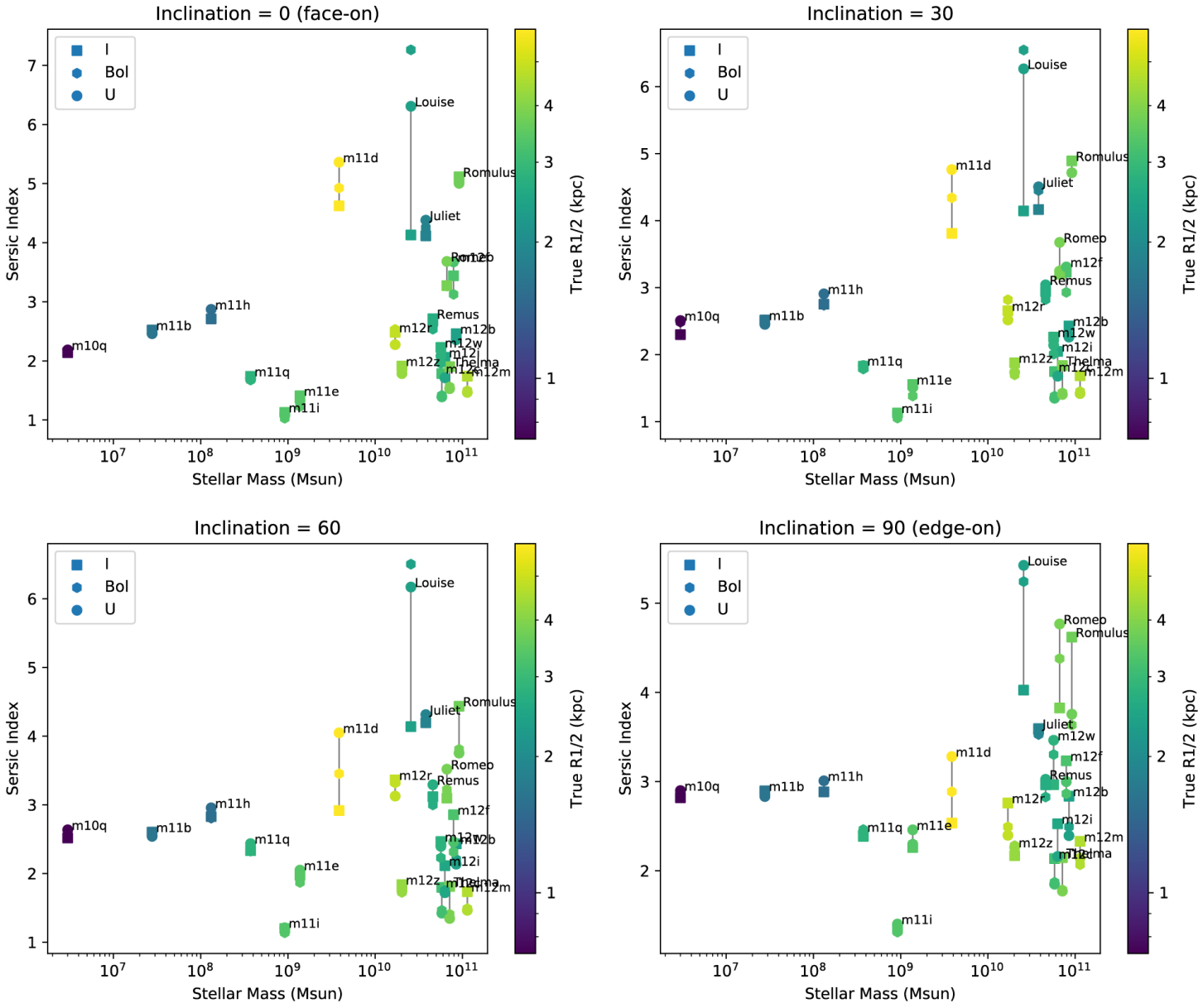

Supp Figure 9.

Scatter plot of Sersic index (horizontal) against ratio of simulated observational $R_{1/2}$ and true $R_{1/2}$. Each point is a single galaxy at a certain inclination and in a single band, so there are 21*4*3=252 total points. This plot shows that at high Sersic index, the accuracy of the $R_{1/2}$ prediction is off compared to that at lower indices. In this plot, red points are galaxies in the I-band, grey points are galaxies in the Bol-band, and blue points are galaxies in the I-band.